

# **Modeling Heat Transfer in the Eye during Cataract Surgery**

## ***Group Members:***

Sona Akkar

Koonal Bharadwaj

Naweed Paya

Adam Shai

Cornell University – BEE 4530

Prof. Ashim Datta

April 30<sup>th</sup>, 2009

## Table of Contents

|   |    |
|---|----|
| I. Executive Summary                              | 3  |
| II. Introduction and Design Objective             | 4  |
| 2.1 <i>Introduction and Background</i>            |    |
| 2.2 <i>Design Objectives</i>                      |    |
| 2.3 <i>Problem Schematic</i>                      |    |
| 2.4 <i>Governing Equation</i>                     |    |
| 2.5 <i>Boundary Conditions</i>                    |    |
| III. Results and Discussion                       | 8  |
| 3.1 <i>Modeling Heat Generation</i>               |    |
| 3.2 <i>Simulation Results</i>                     |    |
| 3.2.1 <i>Eye at steady state</i>                  |    |
| 3.2.2 <i>Eye with phaco heating</i>               |    |
| 3.2.2.1 <i>Varying power output</i>               |    |
| 3.2.3 <i>Eye with phaco heating and cooling</i>   |    |
| 3.2.3.1 <i>Varying total heating/cooling time</i> |    |
| 3.2.3.2 <i>Varying coolant temperature</i>        |    |
| 3.3 <i>Sensitivity Analysis</i>                   |    |
| 3.3 <i>Accuracy Check</i>                         |    |
| IV. Conclusions and Design Recommendations        | 20 |
| 4.1 <i>Conclusion</i>                             |    |
| 4.2 <i>Realistic Constraints</i>                  |    |
| V. Appendix                                       | 22 |
| 5.1 <i>Input Parameters</i>                       |    |
| 5.2 <i>Technical Details</i>                      |    |
| 5.3 <i>Mesh Statistics and Convergence</i>        |    |
| 5.4 <i>Derivations</i>                            |    |
| 5.5 <i>References</i>                             |    |

## SECTION 1: EXECUTIVE SUMMARY

Cataract surgery is one of the most commonly performed surgical procedures in the world, and it involves using a technique called *phacoemulsification*. With this technique, the cloudy, crystalline lens in the eye is mechanically disrupted using a probe that vibrates at an ultrasonic frequency. However, this vibrating tip mechanism leads to frictional heat generation, which can potentially cause extensive thermal damage to fragile tissue structures surrounding the lens. In order to minimize damage due to this frictional heat, a coolant is typically used while the phaco probe is in operation.

In this report, our goal is to model heat transfer in the eye using COMSOL Multiphysics software in three different scenarios: (1) under normal physiological conditions, (2) considering only the frictional heat generation from the phaco probe, (3) and considering both heat generation as well as heat removal by the coolant.

Using a 2-D axisymmetric geometry to model the eye structure, we determined that using the heat source by itself results in temperatures far above the threshold of 328 K for thermal wound injury. However, with the addition of the coolant for heat removal, temperatures in the iris were lowered to less than 320 K, thereby reducing any thermal burn risk to the patient. Further analysis demonstrated that decreasing the coolant temperature or decreasing the probe's operational power can significantly improve the safety of the procedure.

**Key words:** cataract surgery, phacoemulsification, frictional heat generation

## SECTION 2: INTRODUCTION AND DESIGN OBJECTIVES

### *2.1 Introduction and Background*

#### *Cataracts and Cataract Surgery:*

Cataracts are the leading cause of vision loss in adults, age 55 and older, and the leading cause of blindness worldwide. By age 65, about half of the human population has a cataract, and by age 75, almost everyone has a very high chance of developing a cataract. However, cataracts are highly treatable these days as a result of modern advances in medicine, and it is becoming increasingly easier for patients to get full restoration of their vision.

Some of the factors that cause acquired cataracts include exposure to ultraviolet light, trauma to the eye, systemic diseases such as diabetes, and toxins. In fact, the normal process over time of the lens becoming less resilient, less transparent, and thicker can also contribute to the formation of cataracts. It should be noted, however, that age-related cataracts develop very slowly and painlessly. In fact, most people may not even realize that their vision is changing until they find themselves going to the eye doctor seeking a change in eyeglass or contact lens prescription. But in general, blurry or dim vision, colors appearing faded, poor night vision, halos appearing around lights, and sensitivity to bright lights can all be symptoms of a cataract.

Although stronger eyeglasses or brighter lighting may help relieve symptoms of a cataract in the early stages, surgery is the only cure and the most common form of treatment. In fact, more than 3 million people undergo this vision-saving procedure each year in the U.S. alone. Cataract surgery is a simple operation where a surgeon removes the eye's clouded natural lens and replaces it with an artificial, intraocular lens (IOL). The entire procedure is generally done on an outpatient basis and usually lasts between 15 and 30 minutes. Patients may experience little to no pain and can usually return to their normal activities the following day if everything goes according to plan.

#### *Phacoemulsification:*

The usual technique used for cataract surgery is called *phacoemulsification*. This procedure involves incising the anterior lens capsule (about 3 mm long), prolapsing the lens nucleus into the anterior chamber, inserting an ultrasonic probe with an aspirator through a small limbal incision, fragmenting the lens, and aspirating lens fragments from the eye.<sup>1</sup> The phacoemulsifier probe has a steel or titanium tip that vibrates at an ultrasonic frequency of approximately 40 kHz to fragment the lens.

The surgeon first focuses the probe tip (needle) on the cataract's central nucleus, which is denser. While the cataract is being emulsified, it is simultaneously aspirated through a small hole in the needle. The phaco probe also has an incompressible sleeve placed over the needle, which serves as an insulator. Balanced salt solution (BSS), which flows either between the sleeve and the needle or in a separate probe, acts as a coolant that helps prevent burns to the cornea and surrounding eye tissues (Figure 1).<sup>1</sup>

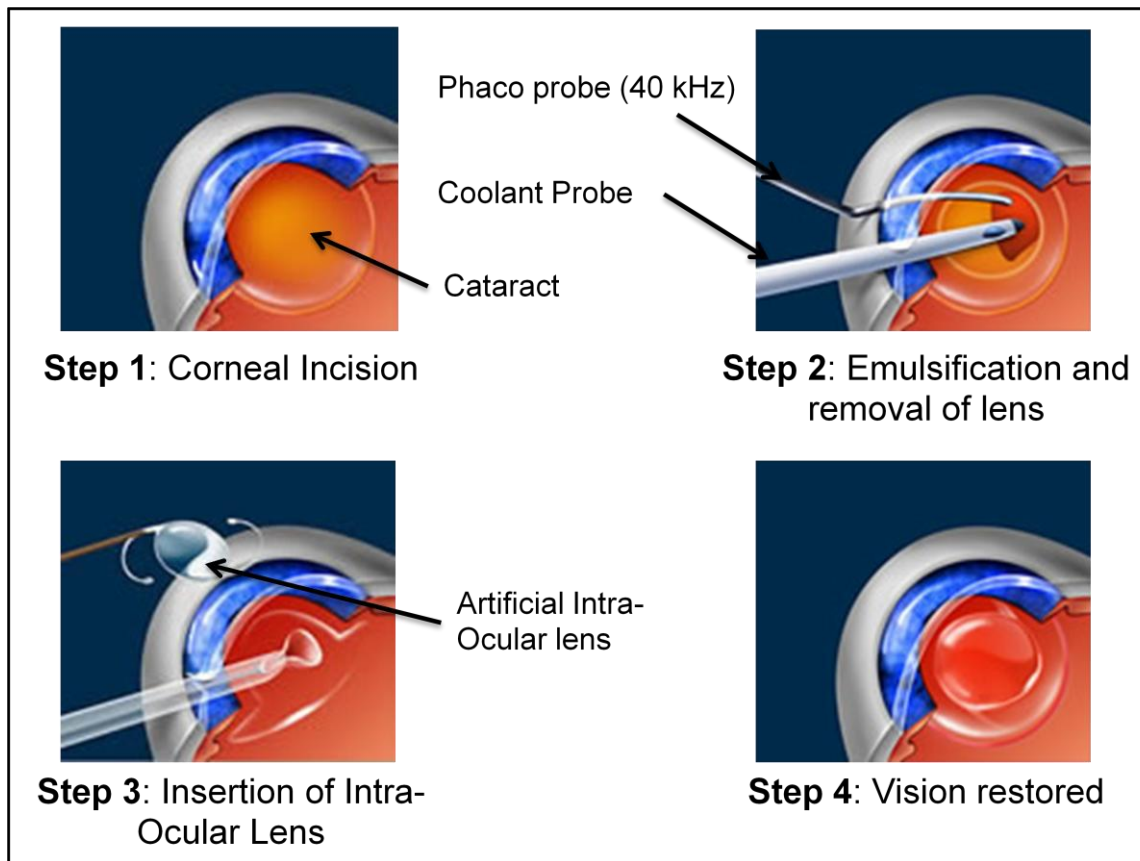


**Figure 1: Step-by-step phacoemulsification procedure<sup>3</sup>**

#### Heat Generation and Dissipation During Phacoemulsification:

The tip of the phacoemulsificator probe oscillates along its greater axis, moving at ultrasonic speed in media of different densities. During this process, its distal extremity fragments the material of the crystalline lens and everything else it comes into contact with. The tip, therefore, has a certain amount of energy that is transmitted to the eye structures while it oscillates. For the most part this energy is used to fragment the lens and to a lesser degree is dispersed as friction or other physical phenomena. Any excess energy that is not used directly to emulsify the crystalline lens is transformed into heat. When the heat can no longer be dissipated and it exceeds a certain threshold, it can damage the surrounding tissues in the eye.

Heat production depends on the coefficient of friction between the contact surfaces. However, it also depends on the dimensions of the surfaces themselves and the speed of oscillation of the tip. In other words, it depends on the power used and, in this case, doubling the power means quadrupling the heat produced!<sup>3</sup>

The heat dissipation system in the phacoemulsificator is based on infusion, which draws balanced salt solution (BSS) through the inside of the handpiece and along the length of the entire tip. It then enters the anterior chamber where it contributes to maintaining the chamber depth and to removing fragments of the emulsified material. The aspiration system also

contributes to heat dissipation as it collects the liquid in the anterior chamber and transports it away from the site through the tip and the handpiece, this time in the opposite direction.

There is a common belief that cutting during phacoemulsification takes place due to cavitation occurring at the frontal end of the tip. The reality of the situation, however, is that all cutting essentially occurs due to mechanical action, much like during jackhammer usage. In the 90's scientists undertook a very detailed study, which proved conclusively that cavitation plays no useful role in phaco or other cutting ultrasound applications.<sup>3</sup>

## ***2.2 Design Objectives***

Due to the high frequency of the ultrasonic phacoemulsifier tip, heat generation due to friction is a concern since it poses a risk of causing thermal damage to tissue surrounding the lens. In order to prevent extensive heat damage, proper irrigation is required during the phacoemulsification process to convect away the excess heat generated by the ultrasonic probe. In our project, we plan to:

- 1) Model heat distribution in the lens and surrounding structures of the eye during the phacoemulsification process.
- 2) Validate our model using published experimental data for temperature in the lens during cataract surgery and assess the extent of thermal damage to the surrounding tissue.
- 3) Analyze the effects of irrigation on heat dissipation throughout the process to minimize risk of tissue damage.

## ***2.3 Problem Schematic***

Based on rotational symmetry of the eye structure as well as comparisons with similar published studies, we formulated our model using a 2D-axisymmetric geometry. Almost all major ocular tissue structures and liquid areas were included in the model, including proper distances of each from the center of the eye, to create a highly accurate and robust model (Figure 2). All structures, including liquid regions, had different material properties associated with them and this data was obtained from past publications. The entire eye was initially set at 37°C, which is roughly the average body temperature. The governing equation, boundary conditions, initial conditions are listed below, and corresponding material properties can be found in the Appendix A. Simulations were then performed in COMSOL Multiphysics, a computational heat transfer and fluid dynamics software.

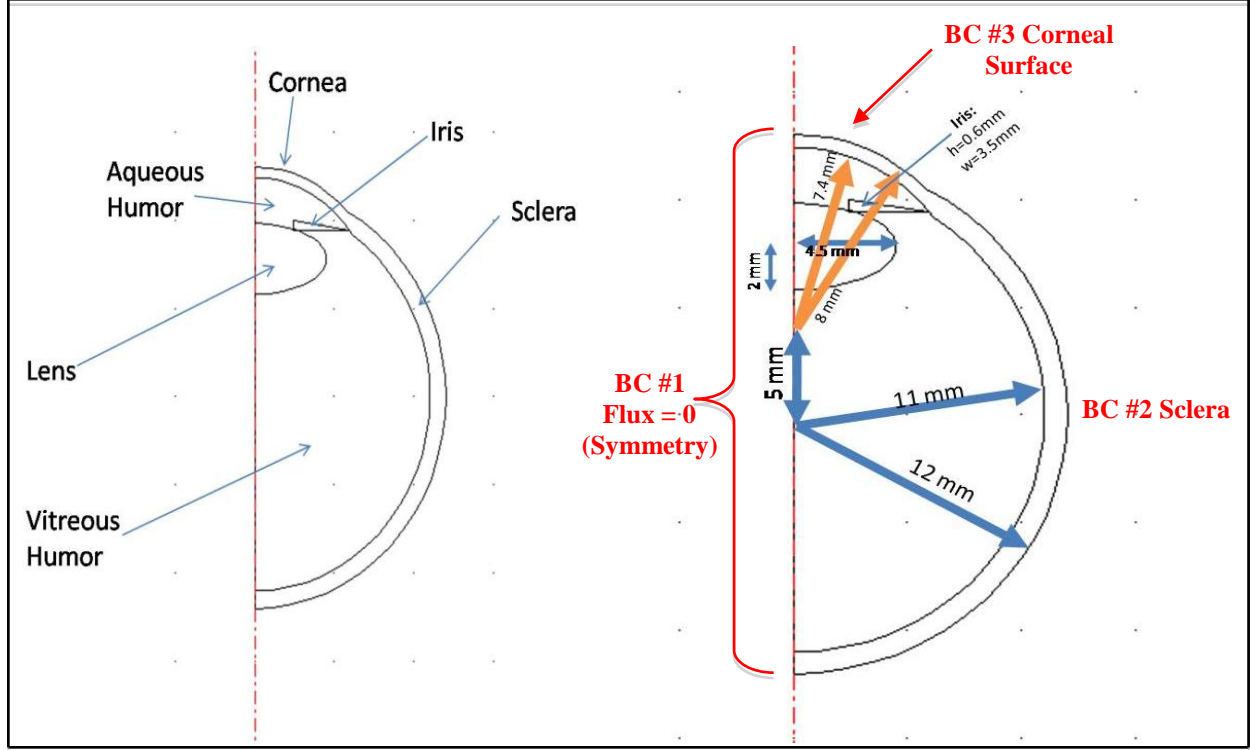


Figure 2: Schematic of internal structures of the eye. Model is 2D-axisymmetric.<sup>12</sup>

## 2.4 Governing Equation

The governing equation solved by COMSOL for this 2D axisymmetric problem is the generalized heat transfer equation in cylindrical coordinates without the convection term. In our model, convection is disregarded because it does not play a significant role in heat transfer within the eye. In addition, frictional heat generation by the probe is modeled using a positive heat generation term and heat removed by the coolant is modeled using a negative heat generation term. Details regarding the derivations of these terms can be found in Appendix D. This approach of using constant values for heat generation and removal is appropriate in this case because we are only concerned with the effective (time-average) thermal effects for the duration of our simulation.

$$\rho C_p \frac{\partial T}{\partial t} = \frac{k}{r} \frac{\partial}{\partial r} \left( r \frac{\partial T}{\partial r} \right) + k \frac{\partial^2 T}{\partial z^2} + Q_{probe} - Q_{coolant}$$

## 2.5 Boundary Conditions

There are a total of three different boundaries in our geometry, which must be handled independently. The details for each boundary are shown below:

*BC #1 – Symmetry:* Vertical axis, heat flux = 0

*BC #2 – Blood heating source on the sclera:* The outer tissue surface of the eye, or the sclera, has blood at body temperature flowing over it. This is given by the boundary condition below, where heat conduction is equal to convection at the tissue-blood boundary.

$$-k\left(\frac{\partial T}{\partial n}\right) = h_{bl}(T - T_{bl})$$

*BC #3 – Corneal Surface:* The outer surface of the eye, cornea, is subject to radiation (electromagnetic), convection (naturally occurring airflow), and evaporation (from tears). The boundary condition below relates the heat conduction out of the cornea to radiation, evaporation and convection.

$$-k\left(\frac{\partial T}{\partial n}\right) = h_{amb}(T - T_{amb}) + \sigma\epsilon(T^4 - T_{amb}^4) + E$$

| Variable      | Property                        | SI Units   |
|---------------|---------------------------------|------------|
| $Q_{probe}$   | Heat generated by probe         | $W/m^2$    |
| $Q_{coolant}$ | Heat removed by flowing coolant | $W/m^2$    |
| $h_{bl}$      | Blood convection coefficient    | $W/m^2K$   |
| $T_{bl}$      | Blood temperature               | K          |
| $k$           | Thermal conductivity            | $W/mK$     |
| $h_{amb}$     | Ambient convection coefficient  | $W/m^2K$   |
| $T_{amb}$     | Ambient temperature             | K          |
| $\sigma$      | Stefan-Boltzmann constant       | $W/m^2K^4$ |
| $\epsilon$    | Emissivity of cornea            | ---        |
| $E$           | Evaporation rate                | $W/m^2$    |

**Table 1: Explanation of the variables used in the heat transfer equation and boundary conditions with their corresponding SI units**

## SECTION 3: RESULTS AND DISCUSSION

### 3.1 Modeling Heat Generation

In order to accurately model frictional heat generation in the lens due to phacoemulsification, we assumed that movement of the phaco probe throughout the lens could be modeled by a heat source term applied to the entire lens. This assumption is valid because during the surgical process, the phaco probe is repeatedly moved across the entire lens surface to mechanically disrupt the structure for removal. This in turn implies that we cannot accurately choose a single point of application of the phaco probe (or heat generation); instead a time-average must be



considered. And since the probe spends equal amounts of time at almost every point in the lens on average, it is appropriate to assume that heat generation takes place in the entire lens.

We further simplified our model by disregarding physical fracturing of the lens and how that may affect the heat transfer, since that would be beyond the scope of this analysis. Another concept utilized in our analysis was “Effective Phaco Time” or EPT. The ability to dynamically adjust phaco power and change power modulations creates tremendous variability in ultrasound delivery during an individual case. EPT attempts to quantify this by expressing what the equivalent phaco time would have been in continuous mode with 100% power. For instance, 2 minutes of continuous (100% duty cycle) phaco time using 25% power would give a 30-second EPT. Switching to pulse mode (50% duty cycle) would give an EPT of 15 seconds. Using hyper-pulse mode (33% duty cycle) would give an EPT of 10 seconds.<sup>10</sup>

Using this approach, an effective phaco time of 10 seconds<sup>1</sup> and maximum probe power of 7 Watts was used. With this information, we calculated the effective source heat generation and used it as an average over the entire lens volume (26,111,358 W/m<sup>3</sup>).<sup>3</sup>

### **3.2 Simulation Results**

#### **Modeling a Typical Human Eye at Steady State**

Modeling the eye under normal physiological conditions, without any external heat source, shows a maximum temperature of 310 K, observed near the sclera. The lens temperature falls between 309.4 K and 309.8 K, a narrow range that is very close to body temperature. Boundary conditions force the small temperature gradient seen around the cornea. In this case, there are three boundary conditions, which govern our system. The first one is that the temperature has to be continuous at the inner boundary. This boundary condition is due to the symmetry of our system (radially axisymmetric) and takes the form of the derivative of temperature vanishing at those points. The second boundary condition is that the cornea experiences heat transfer in the form of radiation, evaporation of tears as well as convection from the ambient air. The third boundary condition applies to the remaining walls of the eye (Figure 3). There, heat from blood flow is taken into account with the convective heat transfer boundary condition. Modeling the typical human eye at steady gives us a baseline for comparison when heating and cooling effects are considered during phacoemulsification. It also allows for an assessment of thermal damage based upon the internal temperatures seen in various anatomical structures before heating, after heating, and with varying coolant properties.

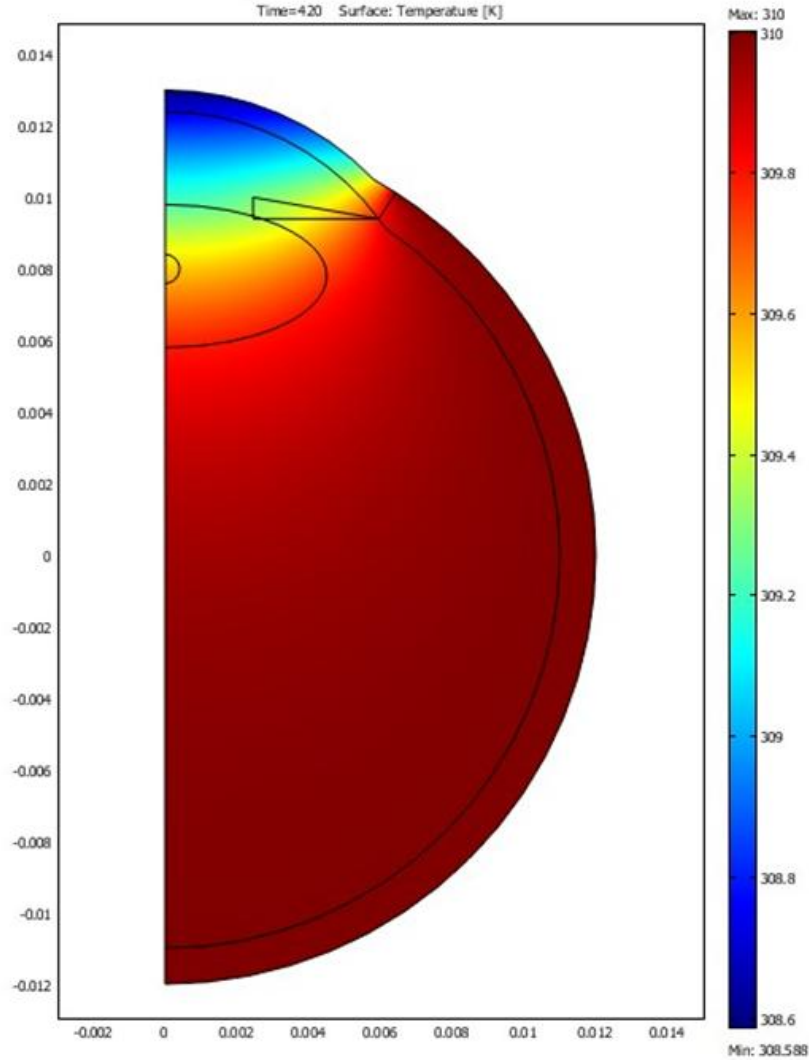


**Figure 3: Modeling of a typical human eye at steady state with no heating or cooling**

### Modeling the Eye with Phaco Heating

When the heat source due to friction from the probe ( $Q_{\text{probe}}$ ) is introduced, which we calculated to be approximately 7 W, the temperature at the center of the lens increases dramatically to a maximum of 364.8 K (Figure 4).

However, since the lens is removed as part of the cataract surgery protocol, high temperatures can be tolerated there. Instead, we are actually more interested in temperatures observed directly adjacent to the lens in other tissues, such as the iris, which are prone to thermal damage. The outer edge of the lens under these conditions jumps to a temperature of 335 K, which is still well above the burn threshold of 328 K.

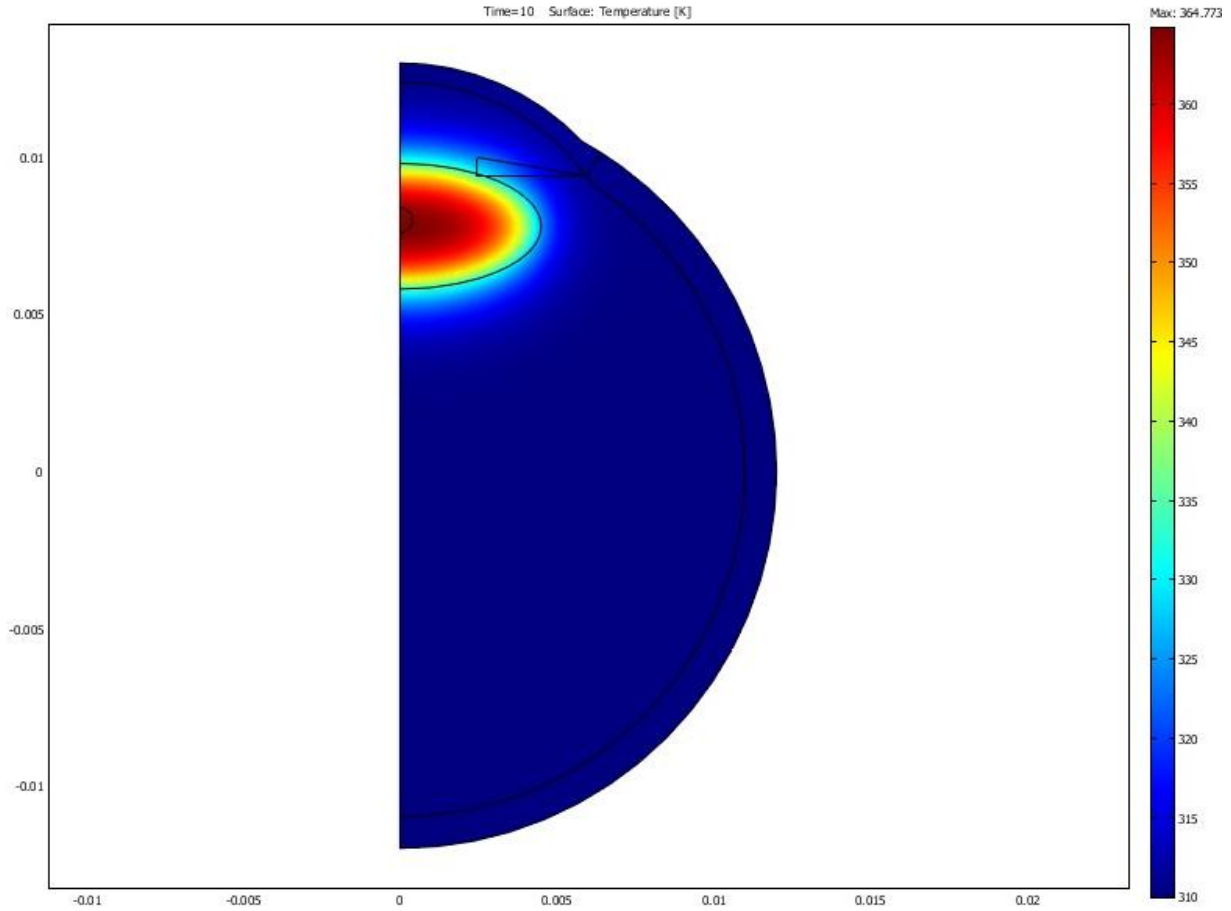


**Figure 4: Modeling of the eye with heating from ultrasonic phaco probe**

### Varying Phaco Power Output

To see the effect  $Q_{\text{probe}}$  has on ocular temperatures, a graph was constructed to relate maximum temperatures in the iris and lens with probe power. As seen in Figure 5, reducing the amount of power that is delivered by the probe leads to a decrease in temperature and raising the probe power likewise leads to an increase in temperature in these two structures. From the observed trend, it appears that the relationship between these two parameters, temperature and power, is essentially linear. The average difference in temperature, when incrementing  $Q_{\text{probe}}$  by 0.5 watts, is 1.61 K in the iris and about 3.91 K in the lens. The linear trend observed here is due to the fact that we only ran the simulation for a relatively small time of 10 seconds, and for such a short time duration the heat equation is dominated solely by the heat generation term.

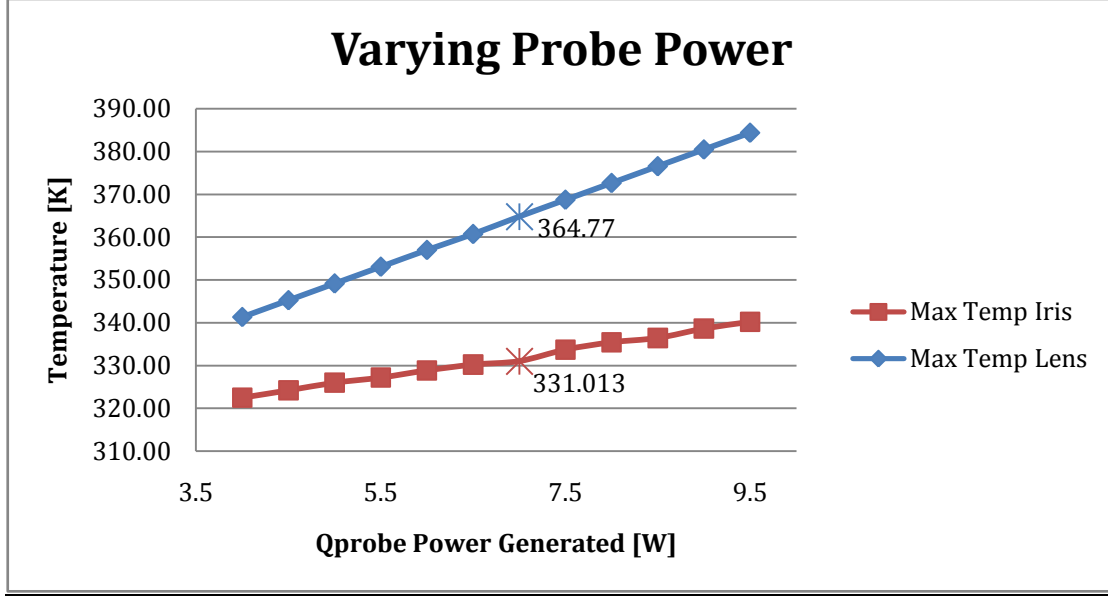


**Figure 5: Maximum temperature in the iris and lens, when the corresponding phaco probe power is adjusted for a 10 second simulation. The star in the iris and lens data indicates the values used in the actual simulation**

### Modeling the Eye with Phaco Heating and Coolant Flow

Phacoemulsification probes have a built-in mechanism for steady coolant flow into the eye to avoid thermal injury during surgery. We modeled the effects of such coolant flow as a convective heat removal term,  $Q_{coolant}$ .

The introduction of this heat removal term reduces the effect of  $Q_{probe}$ , and we are left with  $Q_{net} = Q_{probe} - Q_{coolant}$ . Using  $Q_{net}$  in our model, a new temperature profile of the eye was obtained. In Figure 6, we see that although the maximum temperature in the center of the lens is 342.3 K (above thermal burn threshold), the temperature in the immediate vicinity of the lens decreased to approximately 320 K. Clearly, a temperature reduction of 22 K by the addition of the coolant greatly reduced the risk of thermal injury to the tissue surrounding the lens.

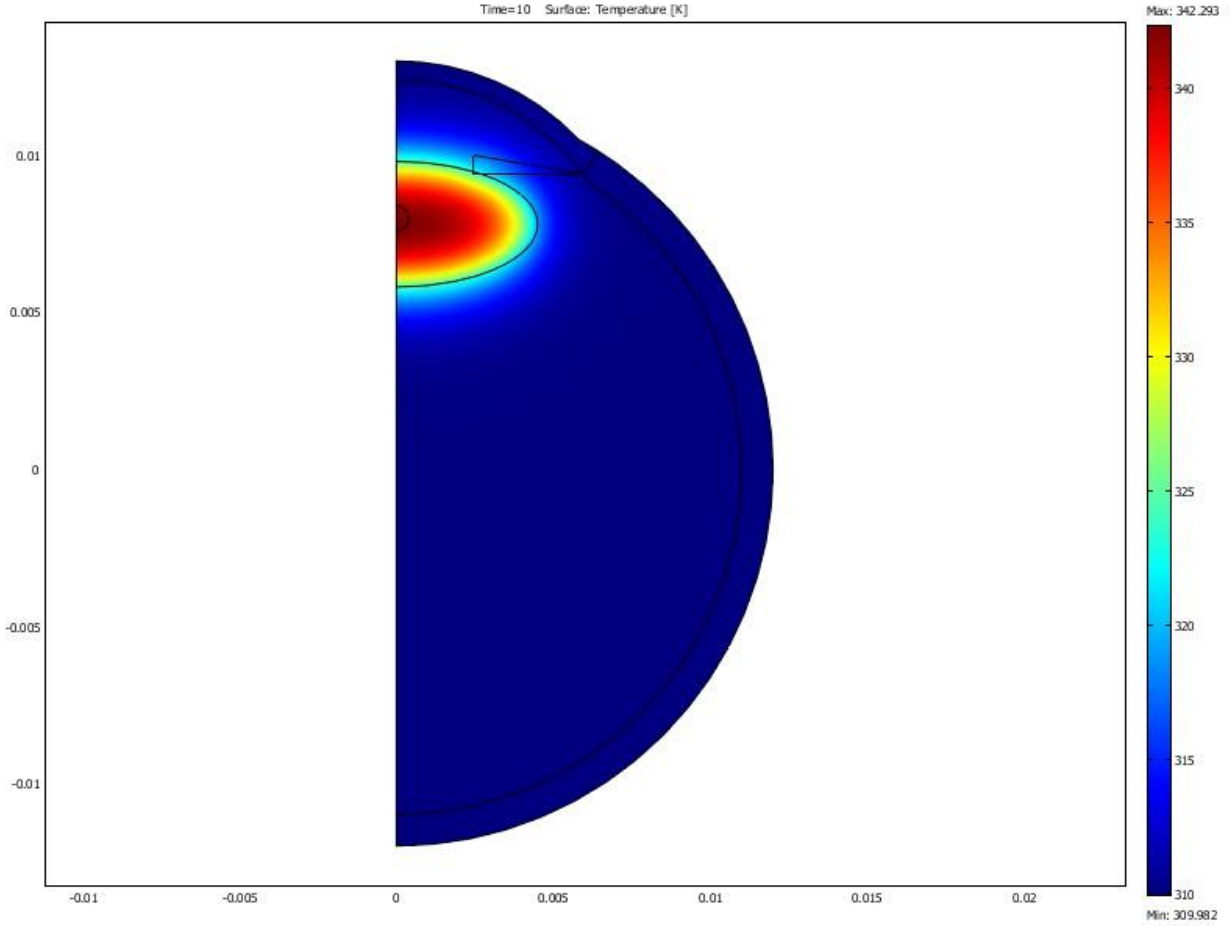


**Figure 6: Temperature profile of the eye considering frictional heat generation and coolant effects**

### Varying Total Heating/Cooling Time

To understand how the effective heat time (EPT) changes the temperature in the computational domain, Figure 7 was created. The maximum temperature was recorded for both the lens and iris for different heating times from 10 – 120 seconds. As the effective heating time was increased, there was also an associated increase in the maximum temperature in both domains. But the spatial characteristics of each structure—distance from the point of heating—demonstrates that each domain was heated a bit differently. Furthermore, as the effective heating time is increased, the distance between both temperature profiles as a function of EPT begins to diverge. The reason for this divergence is that the iris is located farther away than the lens, thereby leading to a greater difference in local temperature gradient for longer times.

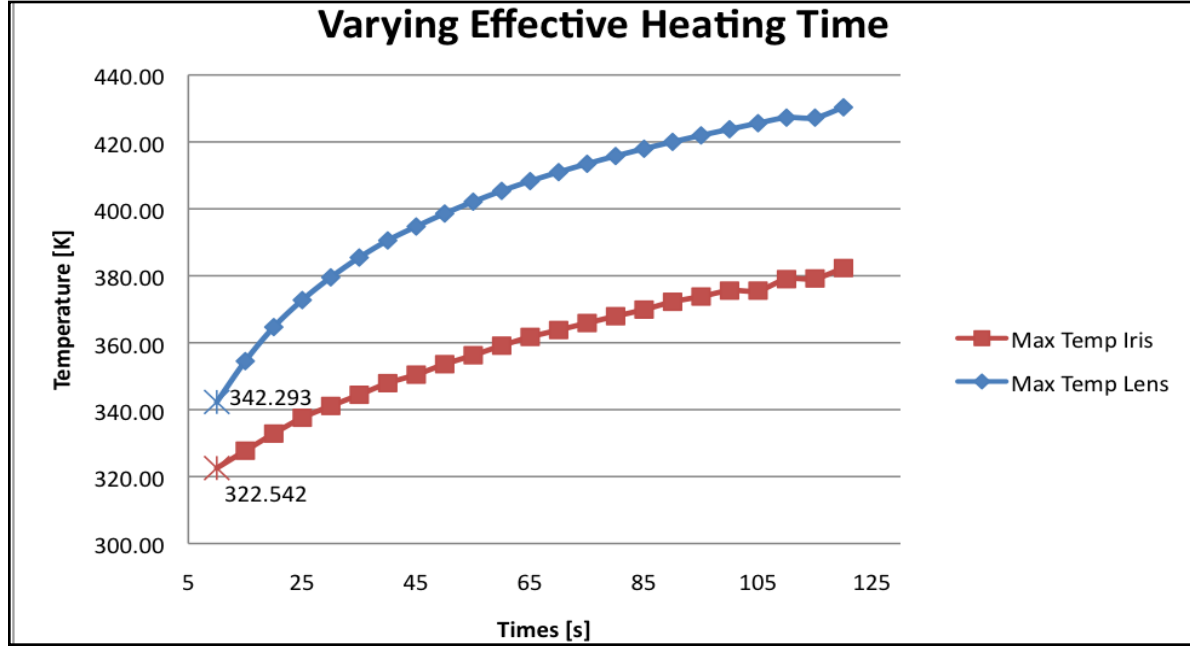


Figure 7: Maximum temperature in the iris and lens when the corresponding effective heating time is adjusted. The star in the iris and lens data indicates the values used in the actual simulation

### Varying Coolant Temperature

One of the parameters which doctors have complete control over during the phacoemulsification procedure is the temperature of the coolant. The temperature of the coolant changes the heat sink term according to the following equation:

$$Q_{coolant} = hA(T_s - T_{\infty})$$

where  $h$  is the heat transfer coefficient,  $A$  is the surface area of the lens, and  $T_s$  is the temperature of the coolant, and  $T_{\infty}$  is the temperature of the lens. We determined the effects of coolant temperature on our model by varying the coolant temperature from 0°C to 40°C, and then running the COMSOL model with the new value of  $Q_{net} = Q_{probe} - Q_{coolant}$ .

To calculate average temperatures, volume integrals were calculated (rotational 2D integrals in our case, since our model is rotationally symmetric) for temperature over specific domains. To get the average temperature we must divide this expression by the total volume:

$$T_{avg} = \frac{\int T dV_{subdomain}}{\int dV_{subdomain}}$$

where  $dV_{subdomain}$  can be either the differential volume of the lens or the eye. Performing these calculations results in data shown in Table 2.

| Coolant Temp (°C) | Integral Lens (K) | Vol. Lens (m <sup>3</sup> ) | Avg. Lens (K) | Max Lens (K) | Integral Iris (m <sup>3</sup> K) | Vol. Iris (m <sup>3</sup> ) | Avg. Iris (K) | Max Iris (K) |
|-------------------|-------------------|-----------------------------|---------------|--------------|----------------------------------|-----------------------------|---------------|--------------|
| 0.00              | 5.55E-05          | 1.69E-07                    | 327.55        | 335.96       | 7.46E-06                         | 2.37E-08                    | 314.94        | 320.13       |
| 5.00              | 5.58E-05          | 1.69E-07                    | 328.97        | 338.06       | 7.47E-06                         | 2.37E-08                    | 315.34        | 320.70       |
| 10.00             | 5.60E-05          | 1.69E-07                    | 330.40        | 340.17       | 7.48E-06                         | 2.37E-08                    | 315.75        | 321.46       |
| 15.00             | 5.62E-05          | 1.69E-07                    | 331.82        | 342.28       | 7.49E-06                         | 2.37E-08                    | 316.15        | 322.43       |
| 20.00             | 5.65E-05          | 1.69E-07                    | 333.24        | 344.39       | 7.50E-06                         | 2.37E-08                    | 316.56        | 323.42       |
| 25.00             | 5.67E-05          | 1.69E-07                    | 334.67        | 346.49       | 7.51E-06                         | 2.37E-08                    | 316.96        | 324.74       |
| 30.00             | 5.70E-05          | 1.69E-07                    | 336.10        | 348.60       | 7.52E-06                         | 2.37E-08                    | 317.37        | 325.59       |
| 35.00             | 5.72E-05          | 1.69E-07                    | 337.52        | 350.71       | 7.53E-06                         | 2.37E-08                    | 317.77        | 325.92       |
| 40.00             | 5.74E-05          | 1.69E-07                    | 338.94        | 352.81       | 7.54E-06                         | 2.37E-08                    | 318.18        | 326.72       |
| No Coolant        | 5.88E-05          | 1.69E-07                    | 347.02        | 364.75       | 7.60E-06                         | 2.37E-08                    | 320.47        | 331.11       |

Table 2: Table showing maximum and average temperatures in the lens and iris considering variable coolant temperatures

The *No Coolant* in Table 2 refers to the case where  $Q_{\text{coolant}}$  vanishes and  $Q_{\text{net}} = Q_{\text{probe}} = 7 \text{ W}$ . The graphical representation of this data is shown below:

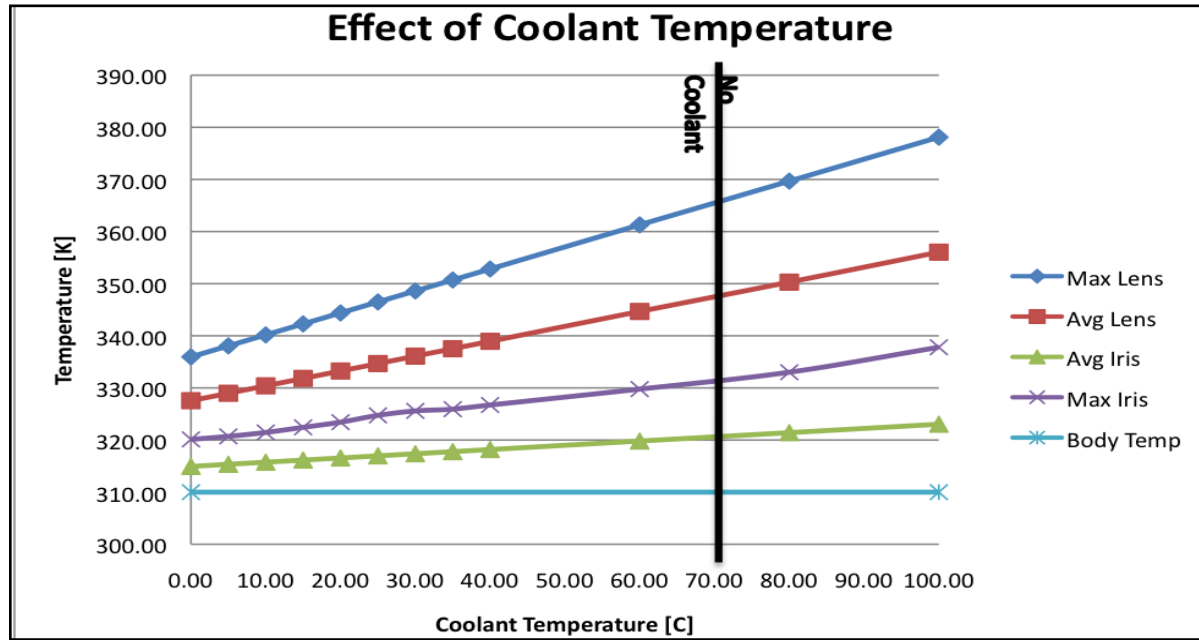


Figure 8: Temperature in various domains of the eye versus Coolant temperature

The vertical line in Figure 8 represents the data for the No Coolant case, which is exactly equal to the case where the temperature of the coolant is equal to  $T_{\infty}$ . The reason for this is that in our model we have chosen  $T_{\infty}$  to be the average temperature in the lens during the entire simulation for the case with 15°C coolant temperature. When the coolant temperature equals this average temperature, there is no extra heat transfer term, a simplification that was made and is discussed

in the Appendix C.

It is also of interest to note that as coolant temperature increases, differences between the lens and the iris increase. In other words, lower coolant temperatures act to decrease the spatial gradient of temperature. A related consequence is the difference between maximum and average temperatures in both the iris and the lens. This difference gives some gauge of the variability of temperature in that area. Because the iris is farther from the heat source than the lens, this variability is always smaller. The conclusion from this piece of data is that the temperature increase drops off quickly from the heat source, as you get further away.

### ***3.3 Sensitivity Analysis***

Our sensitivity analysis with respect to density, thermal conductivity, specific heat,  $Q_{\text{probe}}$ , and  $Q_{\text{coolant}}$  yielded a maximum temperature change of  $\pm 10^\circ\text{C}$  when said parameters were altered by  $\pm 10\%$ . The maximum temperature in the lens was recorded at the end of each simulation (10 sec) as opposed to the average temperature, because maximum temperature in this case is more indicative of tissue damage.

The largest change in temperature was associated with changes in  $Q_{\text{probe}}$  and the density of the lens. The first result seems intuitively obvious; increasing the power output of the probe implies an increase in volumetric heating and thereby results in an increase in the maximum temperature. It is not so obvious, however, why changes in density have such an impact. Nevertheless, an analysis of published literature shows that, in fact, greater phaco probe power levels are generally used when performing phacoemulsification on patients with Grade 4 or Grade 5 cataracts as compared to those with Grade 1 or Grade 2 cataracts.<sup>3</sup> This can be explained by the fact the density of a cataract is directly proportional to its classification grade. In other words, a Grade 4 cataract is much denser than a Grade 2 cataract. Therefore, since denser cataracts give lower maximum temperatures as shown by our sensitivity analysis, it makes sense that greater phaco probe power levels are required to achieve the same temperature change in these cases.

In contrast to  $Q_{\text{probe}}$ , we see the inverse effect for the volumetric cooling term. This result is also makes sense intuitively; a larger cooling term leads to a decline in maximum temperature. Furthermore, by increasing the thermal conductivity the maximum temperature decreases, because more heat is conducted away from the lens. Overall, our sensitivity analysis shows that there isn't a single dominant factor in our simulation. Instead, the effects of a phacoemulsification procedure are dependent on a harmony between the various parameters, Figure 9.



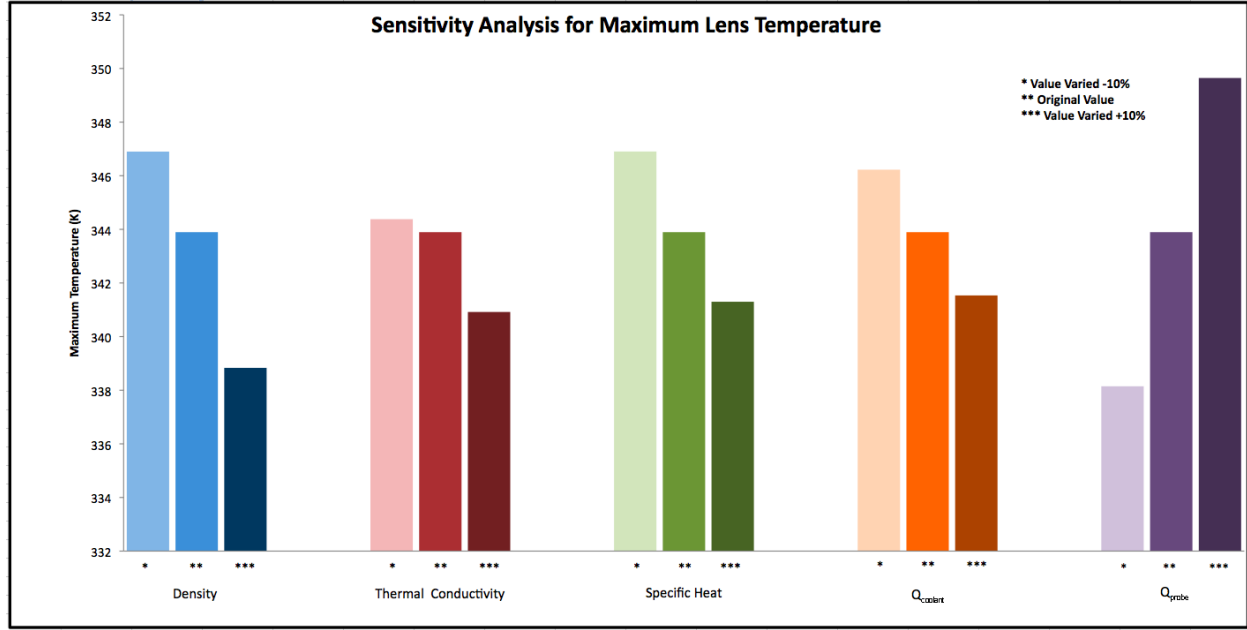


Figure 9: Sensitivity analysis for various parameters used in phacoemulsification modeling

### 3.4 Accuracy Check

In this study, an accuracy check is especially important since our computational model uses effective applications of the heat during sonifications, instead of a more accurate treatment which would use pulse durations and longer time intervals (as well as a smaller and moving heat source). Benolken et al.<sup>11</sup> studied temperature profiles of the eye during phacoemulsification of cat eyes. We used these published thermistor temperature values to make sure our simplifying assumptions did not affect the reality of our results obtained in COMSOL. It is important to note the conditions in which the Benolken experiment took place, however, which might make it different from a more standard phacoemulsification procedure. For instance, neglecting differences between the eyes of cats and the eyes of humans, Benolken et al. took temperature readings only after the lens was completely emulsified so that temperature sensors could get into the eye easily. Additionally, their experiment was conducted under conditions of “stop-flow,” where the eye was first irrigated with coolant and then heated by the phaco-probe. The significance of these differences and their effect on resulting temperature profiles in the eye is not completely known.

Benolken et al. found that with a standard probe tip, a temperature of 66.7°C was the maximum observed at the incision site less than 1mm away in the stop-flow conditions with 25°C coolant flow (Figure 10b).<sup>5</sup> Figure 10(a) shows temperatures we obtained from simulation at points 1mm to 3mm away from the heat source as blue to purple lines respectively, over the course of 90 seconds. In accordance with the stop-flow procedure, we used a simulation with no coolant and 100% power (40 kHz probe), over the course of 90 seconds. In the experimental case, temperatures at 1mm away from the heat source range from about 30 to 70°C. In our simulations, the comparable temperatures range from about 36 to 80°C. At a distance of 3mm away from the heat source, experiments show ranges from about 30 to 62°C, while in our simulation the corresponding temperatures range from about 36 to 65°C. There is a certain

amount of variability in the actual experimental procedure which cannot be accounted for, as well as differences between human and feline eyes. However, it is promising that the results are similar. It is also important to notice the rapid decrease of temperature as distance away from the phaco probe increases. This effect is seen similarly in the experimental cat studies as well as our computational model.

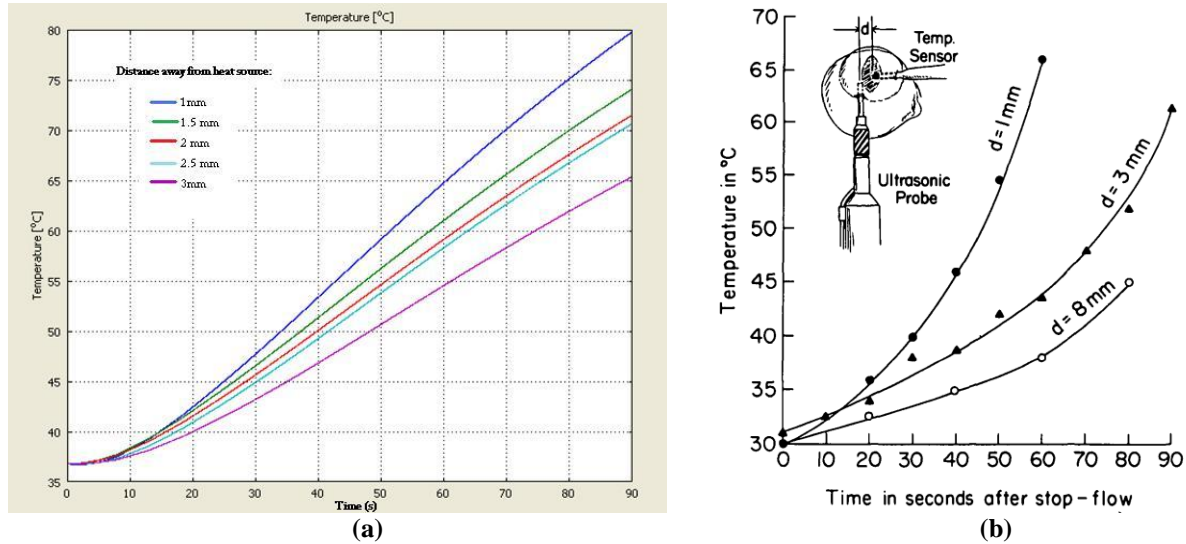


**Figure 10: (a) Temperatures obtained from simulation at points 1mm to 3mm away from the lens (b) Maximum power starts at  $t=0$ . Values of  $d$  specify the distance between the temperature sensor and the fixed position of the sonic probe.<sup>11</sup>**

As a second source of comparison, a study by Corvi et al.<sup>9</sup> was also used. In this study, infrared thermography data of the eye was collected during phacoemulsification procedures (Figure 11). This study being thermographic in nature, however, only provides surface temperature data. It doesn't give any useful information about the inner structures of the eye, which the phaco probe will heat the most, and which are actually the most prone to damage. Because of this drawback of the study, we cannot make a fair comparison of these experimental results to our computations. The highest temperature recorded by Corvi et al. was 44.9°C in an actual phacoemulsification procedure with coolant and probe used at the manufacturer's recommended settings. This temperature corresponds to values, which our study shows in the iris is a considerable distance away from the phaco probe.

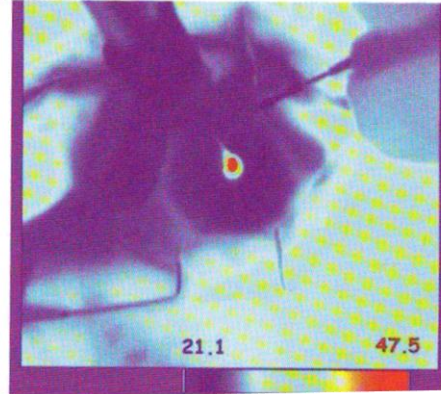


Figure 11: Standard phaco tip with sleeve; max temperature reached 47.5°C<sup>9</sup>

## SECTION 4: CONCLUSIONS AND DESIGN RECOMMENDATIONS

### 4.1 Conclusion

The overall results we obtained clearly show that there is a significant increase in iris temperature when the phaco probe is being used during cataract surgery. During the phacoemulsification process, the ciliary body as well as the iris is in greatest danger of damage due to proximity to the phaco probe. In fact, the maximum temperature in both of these structures reaches 320–330K without any coolant. Hence, it is quite evident that not using any sort of coolant can lead to tissue damage in these areas, especially if the output of the probe and/or time duration of the surgery is increased even slightly.

Coolant flowing over the eye during the phacoemulsification process, however, drastically decreases the amount of heat that approaches the ciliary body and iris. In our model, the coolant solution was forced in to the lens at 20cc/min; this flow rate helps to convect heat away from the critical eye structures. In addition, our sensitivity analysis showed that decreasing the coolant temperature has a reasonable impact upon heat removal.

### 4.2 Realistic Constraints

While COMSOL is a very powerful modeling tool, it cannot recognize design impossibilities that are rooted in the physical reality of the problem. The fact of the matter is that no two surgeons or phaco probes are made alike, and therefore a huge variation is likely to be seen in not only surgical technique, but also the frictional heat generative properties of each individual probe. We assumed that the heat generation is applied over the entire lens, but in reality the probe tip is moving continuously, applying point source heating. Coolant temperatures may also not stay constant once flowing over the lens, even with a constant fluid flow, as it would instantly be heated upon contact. Varying physiological conditions and properties of the patient's eye, coupled with these non-constant conditions make it almost impossible to have our model apply to every situation. We used an effective phaco heating time to attempt to normalize the various surgical techniques and probe variances, but this is an assumption and therefore our model is constrained from truly reflecting reality.

### ***4.3 Design Recommendations***

It can be safely deduced from the modeling results that the temperature of the coolant and the operational power of the probe are two of the most important parameters that need to be carefully evaluated to ensure safety during cataract surgery. Since the general relationship between temperatures in the lens and iris and the probe power is almost linear in nature, the probe power can be adjusted to a convenient and safe level. Using the results from our model, manufacturers and even surgeons can set recommended probe power output levels, based on the length of the procedure, extent of the surgery, and individual properties of the patient's eye.

Also, coolant temperature has an additional effect on the thermal behavior of the phacoemulsification process. Although the relationship between the eye temperatures and coolant temperature is linear, lowering the coolant temperature also drastically decreases the spatial variation of temperature, which is desired for this procedure. The lens would still be heated to a high temperature, but it has to be removed anyway; we are interested in preventing thermal injury to the nearest tissue, which is the iris. From this information, we conclude that lowering coolant temperature would be the most effective method to improve the design of a phaco probe to reduce risk of thermal injury. Phaco probe power may also be decreased, but a lower power may require a longer surgery time, which may lead to additional complications.

### ***4.4 Future Work***

Future work and possibilities to enhance this model would include exploring some of the simplifications we had to make due to the scope of this project and duration of our course. A 3-dimensional model would be the most accurate to use, instead of our 2-D axisymmetric assumption, and this would be the first change to explore. Additionally, phacoemulsification involves not only the phaco probe and the coolant flow, but also a steady aspiration-dispensing tube that is responsible for the discharge and uptake of the coolant liquid. Modeling this phenomenon, using fluid dynamics to simulate real flow parameters, would be ideal to gauge the effectiveness and prevention of burns that the coolant offers. Future models may also be adapted to create a sort of user-friendly platform on which surgeons can input specific parameters of the tools they use (size of probe, wattage, coolant temperature, etc), and obtain an output of recommended surgery time and a risk analysis to better inform their patients of details of the surgery and what to expect.

## SECTION 5: APPENDICES

### 5.1 Appendix A – Input Parameters

Our model subdivided the eye into six distinct domains: cornea, aqueous humor, iris, lens, vitreous humor, and sclera. Relevant parameters for these structures were obtained from Ng et al.

| Parameter     | Value  |
|---------------|--|
| $h_{bl}$      | $65 \text{ W/m}^2.\text{K}$                    |
| $h_{amb}$     | $10 \text{ W/m}^2.\text{K}$                    |
| $T_{amb}$     | $298 \text{ K}$                                |
| $E$           | $40 \text{ W/m}^2$                             |
| $\sigma$      | $5.67 \times 10^{-8} \text{ W/m}^2.\text{K}^4$ |
| $\varepsilon$ | $0.975$  |

Table 2: Parameter values for boundary conditions<sup>4</sup>

| Domain         | Thermal Conductivity [W/m.K] | Specific Heat [J/kg.K] | Density [kg/m <sup>3</sup> ] |
|----------------|------------------------------|------------------------|------------------------------|
| Cornea         | 0.58                         | 3500                   | 1050                         |
| Aqueous humor  | 0.58                         | 4200                   | 1050                         |
| Iris           | 1.0042                       | 3500                   | 1050                         |
| Lens           | 0.4                          | 4200                   | 1050                         |
| Vitreous humor | 0.603                        | 4200                   | 1050                         |
| Sclera         | 1.0042                       | 3500                   | 1050                         |

Table 3: Parameter values for each tissue structure and liquid body within the eye<sup>4</sup>

### 5.2 Appendix B – Solver Details

We used a direct solver (UMFPACK) in COMSOL to obtain the solution. In addition, a time step of 0.01 seconds was chosen to get a reasonably accurate solution without overloading the computer memory. The relative tolerance in this case was set to be 0.01 and absolute tolerance was 0.0010.

### 5.3 Appendix C – Mesh Convergence

In order to confirm the validity of our computations and thereby reduce discretization error, we performed mesh convergence on our model. Since certain ocular structures are critical yet much smaller than others, such as the ciliary body, we had to use a Free-mesh. This approach allowed for an uneven number of discrete elements throughout our model, with a higher concentration in more critical areas.

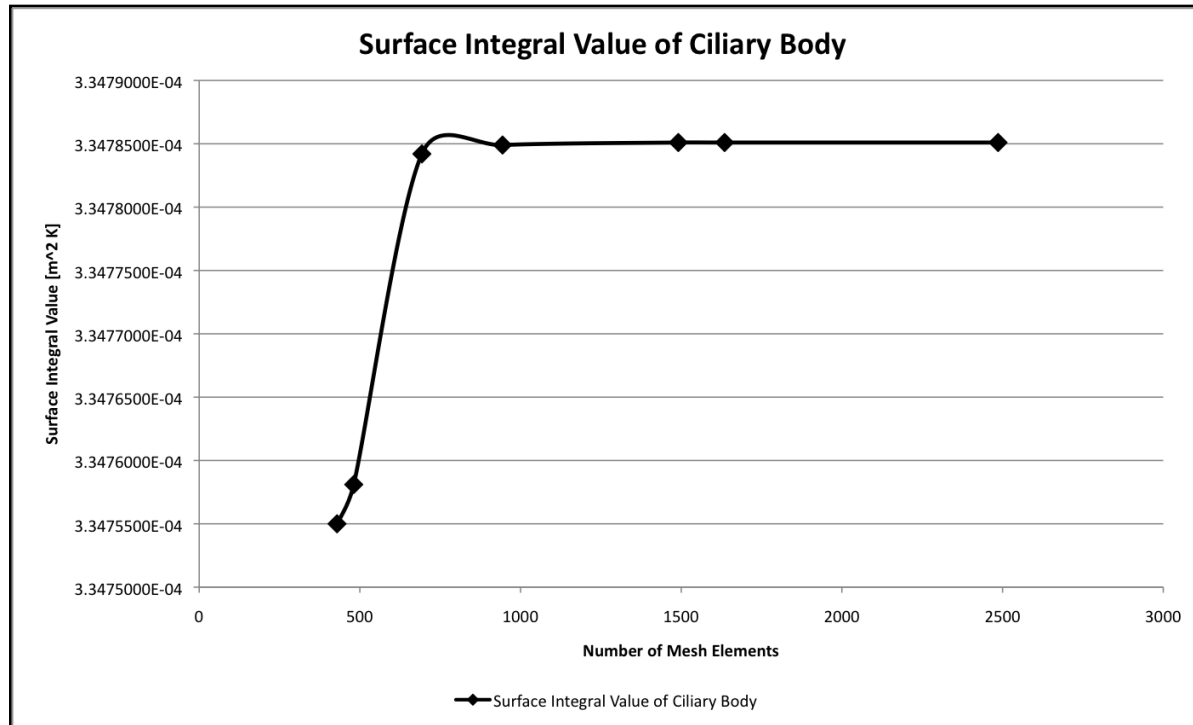


**Figure 13: Mesh convergence using average temperature in the ciliary body**

| Number of elements | Value of Surface Integral at Ciliary Body [m <sup>2</sup> K] |
|--------------------|--|
| 429                | 3.3475500 x 10 <sup>-4</sup>                                 |
| 481                | 3.3475810 x 10 <sup>-4</sup>                                 |
| 693                | 3.3478420 x 10 <sup>-4</sup>                                 |
| 944                | 3.3478490 x 10 <sup>-4</sup>                                 |
| 1491               | 3.3478510 x 10 <sup>-4</sup>                                 |
| 1635               | 3.3478510 x 10 <sup>-4</sup>                                 |
| 2486               | 3.3478510 x 10 <sup>-4</sup>                                 |

**Table 4: Mesh convergence data**

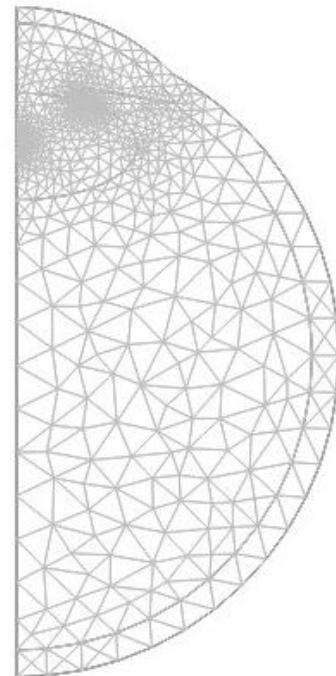


**Figure 14: Free mesh of the eye**

#### 5.4 Appendix D – Calculating $Q_{coolant}$

In order to obtain a value for  $Q_{coolant}$ , we used methods from a previous heat transfer course. The parameter of interest in this case is the convective heat transfer coefficient, which governs energy transfer between the coolant and the eye. Since the coolant is pumped, we have forced convection through a cylinder. In order to calculate the convective heat transfer coefficient, we must calculate both the Nusselt number and Reynolds number, which are parameters of our simulation. The velocity of the coolant flow was taken as 20cc/min, as prescribed in the literature.<sup>3</sup> The density of the coolant was taken as the density of water, and the value for the length was taken as 1.98mm, which is the typical length of the phaco probe tip. To calculate the Reynold's number:

$$Re = \frac{uL\rho}{\mu}$$

$$u = 20 \frac{cc}{min} = 3.33 \times 10^{-7} m^3/s$$

$$L = 1.98 mm$$

$$\rho = 1000 \frac{kg}{m^3}$$

$$\mu = .001 kg/(m.s)$$

$$Re = 214$$

A Reynold's number of 214 is relatively low, and in the case of forced convection through a cylinder, any Reynold's number beneath 2300 is effectively the same. With respect to our simulation, this means that the heat transfer coefficient would vary very little with changes in the parameters of the coolant system. Having calculated the Reynold's number, we move on to calculate the Nusselt number, which for forced convection through a cylinder is given as:

$$\therefore Nu = 3.66 \text{ for } Re < 2300$$

The definition of the Nusselt number relates it to the heat transfer coefficient as follows:

$$Nu = \frac{hL}{k}$$

$$h = k * \frac{Nu}{L}$$

$$k = 0.58 W/mK$$

$$h = 1072 W/m^2 K$$

Using the equation for heat transfer by convection, we arrive at our  $Q_{coolant}$  value:

$$Q_{coolant} = hA(T_s - T_{\infty})$$

$$A = 5.0266 \times 10^{-5} m^2$$

$$T_{\infty} = 15 C$$

$$T_s = 68.32 C$$

$T_s$  was calculated in this case by taking the average temperature over the entire lens for the 10 second duration, and A is the surface area of the lens used in our calculation.

$$Q_{coolant} = \left(1072 \frac{W}{m^2 K}\right) (5.0266 \times 10^{-5} m^2) (53.32 K)$$

$$Q_{coolant} = 2.87 W$$

$$Volume\ of\ the\ lens = \left(\frac{4}{3}\right) \pi r^3 = \left(\frac{4}{3}\pi\right) (4 \times 10^{-3} m)^3 = 2.68 \times 10^{-7} m^3$$

$$Q_{net} = Q_{probe} - Q_{coolant} = 4.13 W = 15393793 \frac{W}{m^3}$$



## 5.5 Appendix E – References

- [1] Kelman, C. D. "Phacoemulsification and aspiration of senile cataracts: a comparative study with intracapsular extraction." *Canadian Journal of Ophthalmology* 8 (1973), 24.
- [2] Hiles, D. A., and Hurite, F. G. "Results of the first year's experience with phacoemulsification." *American Journal of Ophthalmology* 75 (1973), 473
- [3] Phacoemulsification: Principles and Techniques. (Edition 2). Lucio Buratto, Liliana Werner, David Apple, Maurizio Zanini. Slack Incorporated, 2003.
- [4] *Input Parameters:*  
Ng, E. Y. K., and E. H. Ooi. "Ocular Surface Temperature: A 3d Fem Prediction Using Bioheat Equation." *Computers in Biology and Medicine* 37.6 (2007), 829-35.
- [5] *Input Parameters:*  
Ng, E. Y. K., and E. H. Ooi. "Ocular Surface Temperature: A 3d Fem Prediction Using Bioheat Equation." *Computers in Biology and Medicine* 37.6 (2007), 829-35.
- [6] L. J. Bond and W. W. Cimino, Physics of ultrasonic surgery using tissue fragmentation, *Ultrasound in Medicine & Biology*, 22 (1996) p.101-117.
- [7] Chylack LT Jr, Wolfe JK, Singer DM, et al. "The Lens Opacities Classification System III." *Archives of Ophthalmology*, 111, (1993), p. 831-836.
- [8] Brinton, Jason P., Adams, Wesley, MD, Kumar, Rajiv. "Comparison of thermal features associated with 2 phacoemulsification machines." *J Cataract Refract Surg*. (2008) Vol 32.
- [9] Corvi, Andrea. Innocenti, Bernardo. Mencucci, Rita. "Thermography used for analysis and comparison of different cataract surgery procedures based on phacoemulsification." *Physiological Measurement*. 27 (2006), 371-384
- [10] Phaco Chop: Mastering Techniques, Optimizing Technology, and Avoiding Complications. David F. Chang. Slack Incorporated, 2004.
- [11] R. M. Benolken, Jared M. Emery, and D. J. Landis. "Temperature Profiles in the Anterior Chamber During Phaco-Emulsification." *Investigative Ophthalmology and Visual Science*. 13, (1974), 71-74.
- [12] Hwey-Lan Liou and Noel A. Brennan, "Anatomically accurate, finite model eye for optical modeling," *J. Opt. Soc. Am. A*, Vol. 14, No. 8 (1997), 1684-1695.
-